

# Aeroacoustics Effects Generated by the Interaction Rotor-Airframe in a sUAS

Gino Rodrigo Lavagnino Sanchez<sup>1</sup> , Odenir de Almeida<sup>1,\*</sup> , Fernando Martini Catalano<sup>2</sup> 

1. Universidade Federal de Uberlândia  – Centro de Pesquisa em Aerodinâmica Experimental – Faculdade de Engenharia Mecânica – Uberlândia/MG – Brazil.

2. Universidade de São Paulo  – Escola de Engenharia de São Carlos – São Carlos/SP – Brazil.

\*Correspondence author: [odenir.almeida@ufu.br](mailto:odenir.almeida@ufu.br)

## ABSTRACT

Small multirotor unmanned aerial systems (sUAS) have become more accessible and efficient recently, spurring their development for various personal and commercial uses. However, this rapid evolution raises concerns about security, control, and public health due to the proliferation of noisy drones. This study focuses on investigating a major noise source in drones called rotor-airframe interaction, which generates tonal noise through pressure fluctuations and wake interactions. To address this issue, we designed and tested three airframes with varying arm configurations. High-definition microphones and data acquisition systems were employed to measure pressure levels, and MATLAB code helped analyze the data as A-weighted signals to identify noise reduction possibilities. The key finding was that motor noise was a significant contributor, producing multiple pure tones at mid and high frequencies. Additionally, the noise signature was heavily influenced by the arm's geometric shape and angles, underscoring the complex nature of rotor-airframe flow and acoustic interactions.

**Keywords:** sUAS; Aeroacoustics; Noise emission; Rotor-airframe; Turbulence.

## INTRODUCTION

Due to their simple design and programmability for diverse tasks, small multirotor unmanned aerial systems (sUAS), or drones, attract interest from governmental, military, and business sectors. They enhance work efficiency, reduce costs, and mitigate risks in various applications such as fast delivery, accurate tasks in challenging locations, and military operations. As reported by Insider Intelligence (2021), sUAS applications range from surveillance to environmental monitoring and package delivery.

However, the integration of small unmanned aerial vehicles (UAVs) into societal norms requires careful consideration of factors, including challenges and drawbacks. National security, flight control, and noise pollution are among the key concerns. The rotor-airframe interaction, a critical phenomenon shaping the acoustic signature and overall performance of sUAS, is of particular interest. The Federal Aviation Administration (FAA 2022) and European Union Aviation Safety Agency (EASA 2018) view multirotor as significant noise pollutants due to their low altitude of operation and high motor revolutions, producing a distinct high-pitched noise.

The interaction between rotors and airframes in sUAS is characterized by intricate fluid-structure interactions that give rise to aeroacoustic effects. These effects manifest as noise emissions that not only impact the acoustic environment, but also

**Received:** Sep. 15 2023 | **Accepted:** Mar. 19 2024

**Section editor:** Valder Steffen 

**Peer Review History:** Single Blind Peer Review.



This is an open access article distributed under the terms of the Creative Commons license.

potentially hinder operational efficiency, stealth capabilities, and public acceptance of sUAS. Despite the rapid advancement in sUAS technology, a comprehensive understanding of the underlying aeroacoustic mechanisms, particularly in the context of rotor-airframe interactions, remains a compelling yet challenging endeavor.

To date, research in aeroacoustics has predominantly focused on larger rotary-wing and fixed-wing aircraft (Brocklehurst and Barakos 2013; Molino 1982; Roger 2019), with limited attention directed towards the unique characteristics of sUAS. However, the reduced scale and distinctive design of sUAS introduce novel challenges and opportunities in mitigating and managing aeroacoustic effects (Candeloro *et al.* 2022). The compact size, lightweight structures, and increased reliance on electric propulsion systems further underscore the need for targeted investigations into the acoustic signature of sUAS, particularly concerning rotor-airframe interactions.

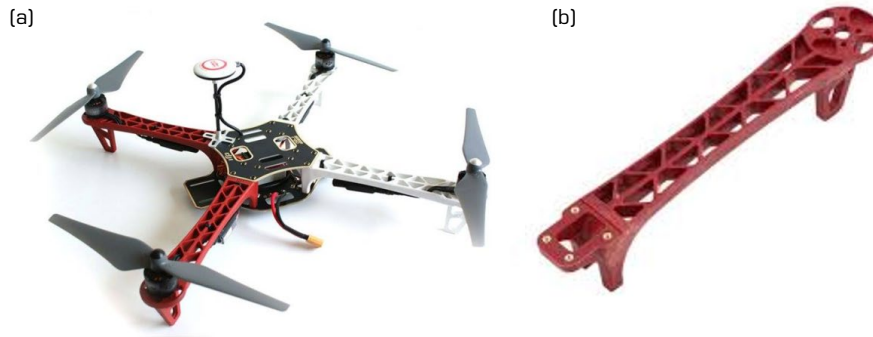
Various papers have been published to explore the source of the noise emission by rotor-airframe interaction. Rapid steps have been taken to examine new concepts of rotors and airframes by changing their format, material, proximity between them and so many other variables that could attenuate the noise generated. The acoustic signature of sUAVs has been described by Candeloro *et al.* (2017), showing a significant sound pressure level (SPL) change for an observer placed underneath the sUAV. A summary of NASA efforts for exploring the acoustics of sUAVs was presented by Kloet *et al.* (2017) and Zawodny *et al.* (2018, 2023), which indicated a 8 dBA overall noise reduction by elevating the rotors from the airframe in forward flight. Detailed aeroacoustic measurements were presented by Kloet *et al.* (2019) for showing the impact of the rotor-airframe orientation. Both numerical and experimental data were used to show that more broadband noise in the low to mid frequencies was presented with the observed placed bottom-mounted under significant influence of the airframe. A numerical approach was presented by Lee and Lee (2020) to evaluate the rotor interactional effects on aerodynamic and noise characteristics, showing that the separation distance between rotor and airframe affects significantly both aerodynamics and aeroacoustics characteristics of such sUAVs. While many studies address the case of hovering flight, the work of Caprace *et al.* (2022) focused on analyzing the effects of rotor-airframe interaction in forward flight by performing large eddy simulation (LES). The results were relevant to show how modern techniques could be used to assess flow field data such as vortex interactions with obstacles for wake characterization purposes as also seen in other works (Jordan *et al.* 2020; Kekus-Kumor and Sieradzki 2023; Whelchel and Alexander 2021).

Moreover, humans can also be affected physiologically by noise pollution from sUAVs and some of consequences can be hypertension, insomnia, cardiovascular problems as related by National Geographic Society (2019). Another important study was performed by Airborne Drones (2020), in which the height of operation dilemma is discussed in rural, urban, and suburb areas to attenuate UAVs noise as much as possible and do not disturb humans and wildlives routine. The work of Watkins *et al.* (2020) raised 10 questions concerning the use of drones in urban environments, showing that there are still steps to be taken for achieving a safe and pleasant environment in terms of drone's operation.

The aim of this research is to chart the SPLs produced by a standard sUAV during typical operation, with a specific focus on characterizing the interaction between the rotor and the airframe. To accurately characterize the sound environment, we conducted tests outdoors under controlled conditions, examining three distinct airframe arms, or holder designs. Our aeroacoustics setup allowed us to investigate sound emissions exclusively from the propeller's plane. In the subsequent sections of this paper, we will delve into our methodology, experimental setup, and the results of our investigation. By shedding light on the intricate interplay between rotor blades and airframe structures, the main contributions of this study are to seek for advanced strategies aimed at mitigating noise emissions in sUAS. Ultimately, the focus was kept to the rotor/arm acoustic interaction by itself to enhance our comprehension of the complex aeroacoustics phenomena and their implications within the rapidly evolving landscape of sUAS.

## Test article

Given that the primary aim of this study is to exclusively examine the aeroacoustics effects resulting from the rotor-airframe interaction, the choice was made to employ an existing commercially available arm and rotor from the Flame Wheel 450 drone (DJI). The visual depiction of the physical model is illustrated in Fig. 1, while simultaneously serving as the default configuration for testing purposes (referred to as Arm-0).



Source: Elaborated by the authors.

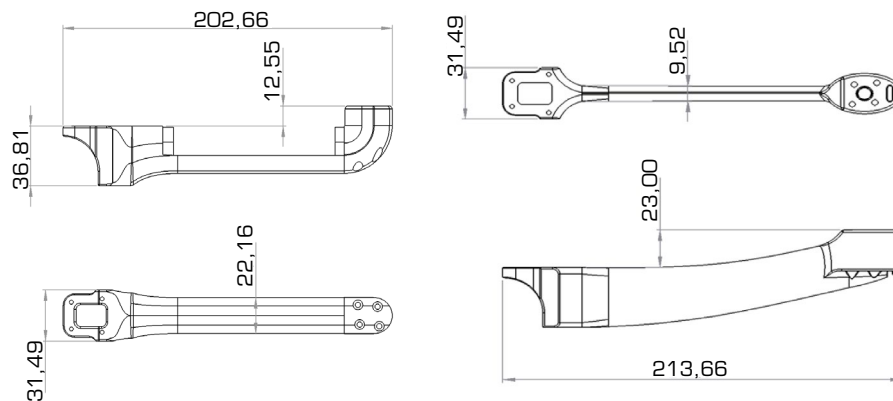
**Figure 1.** (a) Picture of rotor-airframe (DJI F450); (b) Perspective view of Arm-0 configuration.

Inferences from Wang *et al.* (2019) show that by increasing the separation rotor-airframe and lowering the airframe's width to minimize the contact area of the flow against the airframe is critical to reduce the tonal noise. Therefore, the research was conducted, in pursue of an existing airframe project that had one or both characteristics mentioned before, as described in sequence.

### Arm-1 and Arm-2 configurations

Figure 2 shows the physical model with the two configurations (Arm-1 and Arm-2) employed to investigate the flow and acoustic characteristics (dimensions in mm). The vertical distance between the rotor wingtip and airframe of 27 mm, from the original F450, remained constant for the two configurations used in this study. The base for the engine was not modified in both configurations, being the geometric change only applied to the arm structure.

The idea behind the design of Arm-1 was to build an aerodynamic shape as seen in some other drones such as Obsidian Wasp FPV racing frame and Diatone GTX 549. Here, it is important to say that due to the shape of the arm to be exposed to the propeller's wake could enhance or mitigate the noise emission, since no previous study was carried out to check the flow field. The arm itself was designed to be slender and to minimize the obstruction against the flow. In the Arm-2, the idea was to create a porous structure where the flow could interact and additional sound absorbing material could be used to try to attenuate possible tonal noise. Regarding the sound absorber material, it was used a 2 cm beveled eggshell flame-retardant foam for insulation, treatment, and acoustic absorption (MG Foam with  $23 \text{ kg}\cdot\text{m}^{-3}$ ).



Source: Elaborated by the authors.

**Figure 2.** A schematic view of Arm-1 and Arm-2 configurations.

Figure 3 depicts both Arm-1 and Arm-2 final configurations assembled in the test-bench.



Source: Elaborated by the authors.

**Figure 3.** Final assembly of Arm-1 and Arm-2 configurations.

## Operational equipment

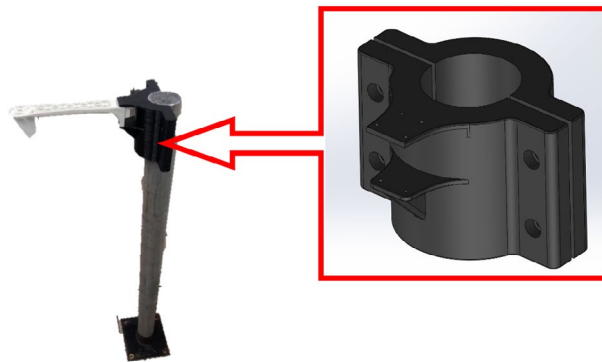
The individual set of the Flame Wheel DJI450 was constituted by the following components: Frame Arm 450FAC named as Arm-0 configuration in this work; Brushless motor EMAX XA2212 1400 Kv; ESC Simonk EMAX 30 A; and HQ Propeller 8' × 4.5'. For the power supply, instead of using the drone default battery it was decided to use a ATX Power Source 500 W to maintain a constant energy supply and do not depend on the capacity and durability of a battery. Also, it is reported by Intaratep *et al.* (2016) that additional noise from the motor/ESC was observed during such kind of measurements. The idea was to eliminate the battery dependance during the tests without adding noise to the system. This approach will be evaluated latter on by showing the background noise levels.

## Experimental setup

This section describes the methods and measurement techniques used in acquiring acoustic data. The rotor-airframe configurations, described in the previous section, were used in three separate test campaigns to obtain the acoustic data. All experiments used rotational speeds varying from 3,000 up to 6,000 rpm.

### Clamp holder structure

To ensure proper positioning of all rotor/airframe configurations and to prevent any potential external interference, a metallic tube-like structure was fabricated using a steel tube with an outside diameter of 100 mm and a height of 1 m. To securely hold the drone's frame and rotor at a specific height, a custom-designed and 3D-printed clamp holder structure was created, considering the airframe's characteristics to ensure a firm hold (Fig. 4). Additionally, during the measurements, the clamp holder structure was fully covered with acoustic foam in an attempt to minimize sound reflections.



Source: Elaborated by the authors.

**Figure 4.** Clamp holder structure.

### Data acquisition equipment

Acquired acoustic data is the basis to analyze a possible solution for noise reduction in the rotor-airframe interaction and to verify the effect of arm design. Acoustic far-field data was acquired using two Bruel & Kjaer Pressure-field ¼" microphones type 4944B. The signal from each microphone was band-pass filtered from 20 Hz to 25 kHz using a Bruel & Kjaer Nexus 2690

signal-conditioning amplifier and recorded using a National Instruments NI 9162 USB Carrier A/D board and MATLAB software for acquisition control. The voltage signals were sampled at 51.2 kHz for 20 s for each test setup. Data was processed by using a discrete Fourier transform (DFT) with a fast Fourier transform (FFT) algorithm being executed in MATLAB code as well. The pressure power spectrum was converted into SPL with units of decibels (dB), where  $P_0 = 20 \mu\text{Pa}$  and  $P$  is the recorded acoustic pressure according to Eq. (1). A-weighting procedure by following normative ISO (2003) was applied in the post-processing of the acoustic data for account for the relative loudness perceived by the human ear. It should be noted that background (quiescent) noise amplitudes were acquired but were not subtracted from the data by following Intaratep *et al.* (2016) procedure. This choice was mostly based on noise levels gathered during the experiment, since most important tonal component part of the spectra were at least 10 dB above average background noise and well perceived during the acoustics measurements.

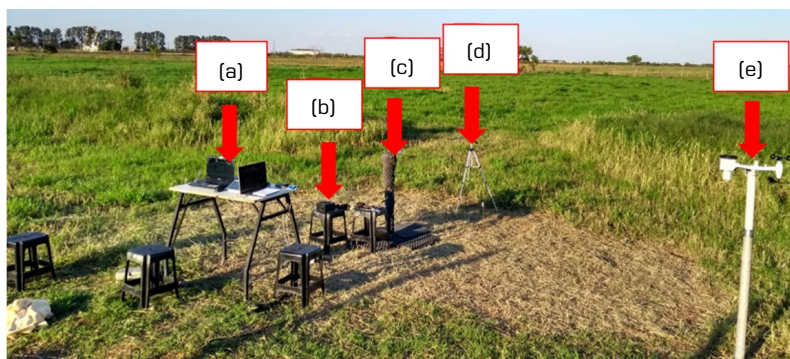
$$SPL = 20 \log_{10} \frac{P}{P_0} \quad (1)$$

The electrical connection between the power supply, ESC and motor was completely checked before the test. To get a right assessment of rotor-airframe interference, it was imperative to maintain maximum freedom within the designated area of interest (upper segment of the airframe) to preempt any potential occurrence of flow disruption or turbulence generation. Consequently, a cable extension measuring approximately 0.60 m (for each cable) was introduced between the ESC and the motor. This extension facilitated the installation of cables beneath the airframe. On the opposite end of the ESC, the energy cable was linked to the power source, while the signal acquisition ESC cable was connected to the MEGA 2560 board. Finally, the MEGA 2560 was interfaced with the computer to enable receipt of commands from the Arduino IDE-Library ESP 8266 and a code was written to perform this task. To ensure this code precision, a test was performed before the set-up, using the Arduino Uno to determine the motor's rpm in relation to the PWM (pulse width modulation) input via computer's keyboard. This was only to set a parameter/range calibration and to obtain a more accurate reading of rpms operating the motor with and without the propeller. A digital tachometer DT-2234C was used to measure and to validate the rpm.

### Outdoor measurements

The test location was an open field on the university premises. This area was devoid of major obstacles near the test arena and had low vegetation (only grass), as pictured in Fig. 5.

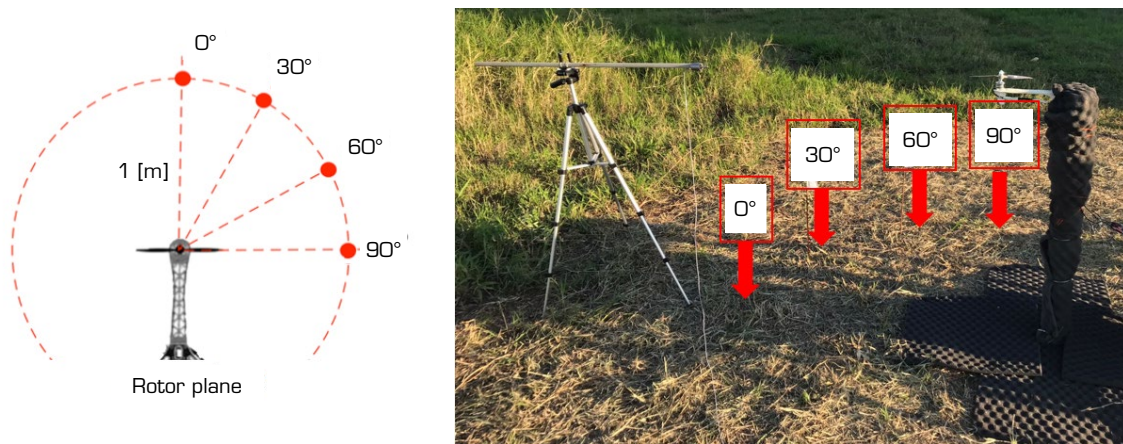
As shown in Fig. 5, after finishing the set up the areas were divided as follows: (a) Data processing center; (b) Power supply; (c) Testing setup; (d) Microphone (acquisition system); and (e) Weather station. The test field area coordinates are (18°56'43'43"S 48°12'36" W – Uberlândia, MG, at 940 m Elevation). Finally, a weather station was set up to collect the environment conditions during the experiment. Wind speed is an important factor that could affect outdoor sound measurement, this is the reason measurements were taken after dawn so wind speed would be less than 1 m/s by following normative ISO 9613-2 (ISO 1996). It is also known that the phenomenon of atmospheric sound absorption can exert an influence on acoustic assessments conducted in outdoor settings. Notably, during the tests the temperature, pressure and humidity did not vary remarkably, and the acoustic data was completed at a temperature of 24 °C, 101.7 kPa of ambient pressure and 30% of relative humidity. The final data were not correct to account for atmospheric sound absorption.



Source: Elaborated by the authors.

**Figure 5.** Field test area (rural area – Campus Glória). (a) Data processing center; (b) Power supply; (c) Testing setup; (d) Microphone stand; (e) Weather station.

A mapping for the different sound receiver angles ( $0^\circ$ ,  $30^\circ$ ,  $60^\circ$ , and  $90^\circ$ ) was marked on the test site, to establish where is the microphone is going to be positioned (Fig. 6). Several studies discuss the concept that noise level is the highest when measured at a 45-degree angle (Oleson and Patrick 1998). In this work, only the sound profile in the in-plane (rotor plane) at the high of 1 m was measured. No measurements were taken underneath the rotor-airframe interaction, mainly due to limitations in the setup. Further improvements are being developed to account for acoustic data underneath the rotor-airframe, since the broadband and tonal noise could be greater than in the in-plane direction as pointed by Oleson and Patrick (1998).



Source: Elaborated by the authors.

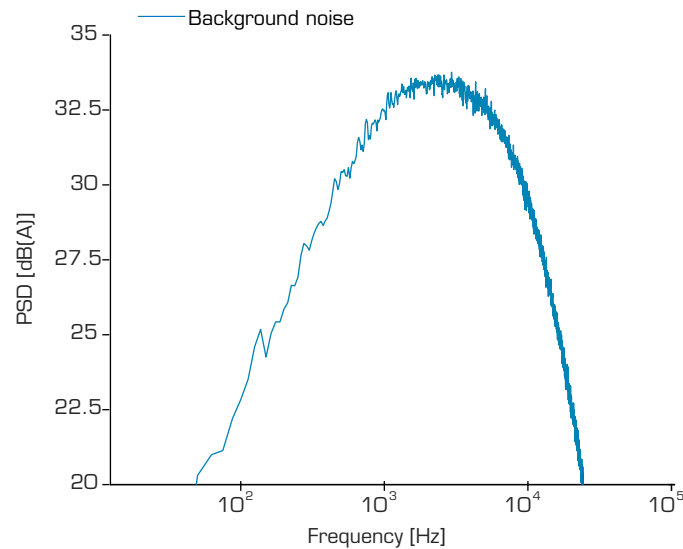
**Figure 6.** Angle mapping referenced in the motor center and actual setup with microphone positioning.

## RESULTS AND DISCUSSION

After processing the data collected through experimental testing for each arm, measurements of pressure levels at various angles during the operation of the drone were obtained. These results are illustrated using A-weighting plots, as previously discussed; this method is employed to filter signals to align with the auditory perception of humans. As is customary in experimental research, potential sources of error were carefully considered. For a more comprehensive and enhanced understanding of the procedure used during the experiment, this section has been subdivided into the following topics: background noise establishment and broadband noise generated by the motor without propeller, results from each arm configuration in the rotor plane, and a comparative analysis of results across all configurations at 4,500 rpm.

### Background noise level

Since the test was performed outdoor, the noise baseline was established through measurements of the background noise present in the area where the setup was mounted. As mentioned, the testing location was a rural area away from external noise interferences such as traffic noise. The test ground was nominally flat and covered with grass. All measurements were taken three times with the microphone placed at a height of 1 m from the ground. All tests were conducted early evening with wind speeds below 1 m/s and with minimal external natural sounds. No atmospheric absorption of sound was considered during the post-processing since the atmosphere was stable during the whole test-campaign maintaining constant the temperature at  $24^\circ\text{C}$ , 101.7 kPa for ambient pressure and 30% of relative humidity. In this quiet ambient at nighttime, the background noise is usually below 35 dBA. Figure 7 illustrates the background noise level measured prior to the main tests. As mentioned before, the background noise was kept low during the whole test campaign with overall SPLs (OASPL) values of around 32 dB. It also important to say that the noise signature of the tested configurations were expressively higher with tonal components well above 10 dB.



Source: Elaborated by the authors.

**Figure 7.** Background noise level measured at test location.

### Engine alone (EA) noise signature

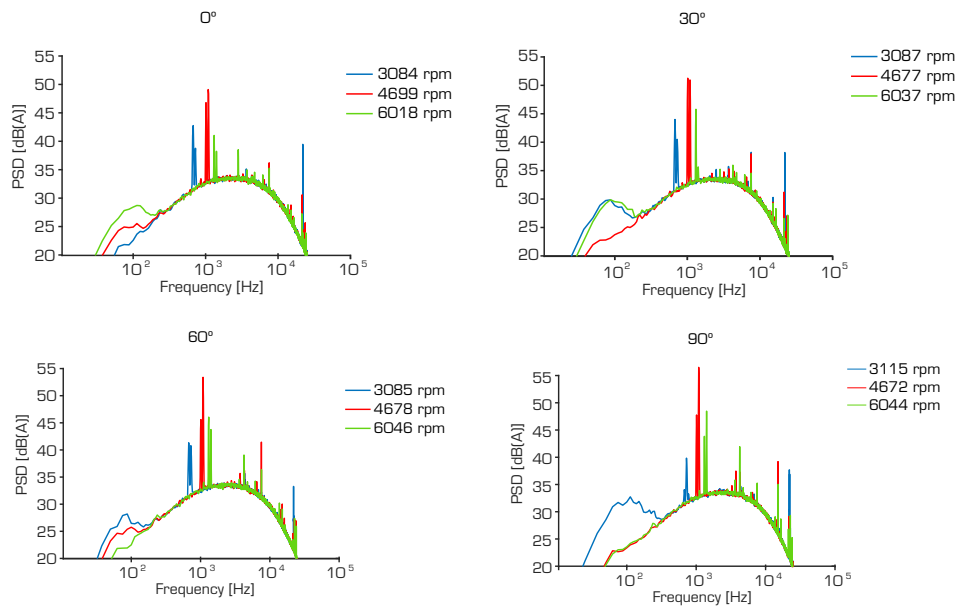
The next step was to perform the noise levels generated by the motor itself, i.e., without the propeller. By following this approach, it is expected to identify and isolate possible noise related to the characteristics of the motor alone and not with the rotor-airframe interaction. These data were acquired for four different angles, with three different rotational speed (rpm). Figure 8 depicts the noise signature for the EA run.

From Fig. 8, it can be observed that the noise was practically equal for each angle, with tonal components well discrete through the narrowband spectra. At approximately 3,100 rpm, a peak frequency around 675 Hz is observed at all angles. A very high content peak frequency is also observed at approximately 21,980 Hz. When running at approximately 4,500 rpm, it is possible to observe a multiple frequency peak at around 1,088 Hz and some other small peaks at 7,550 Hz and 15,100 Hz for angles of 60° and 90°, respectively. Finally, for 6,000 rpm, multiple peak frequency at around 1,313 Hz/1,425 Hz, at 4,238 Hz and at 15,100 Hz were identified. These tonal components were attributed to the mechanical/electrical characteristics of the EA and remains present in the noise signature when the propeller is installed. Also, the appearance of these tonal components will change the sound profile in the rotor plane dependent of the observer angle. The presence of motor noise at both low and mid frequency was also reported by Oleson and Patrick (1998), showing similar trend in tonal components, despite the model and sizing of the motor alone. In summary, a key point for such kind of measurement is to isolate the influence of the motor alone before proceeding with the acoustic measurements for the drone's configuration.

### Sound profile in rotor plane

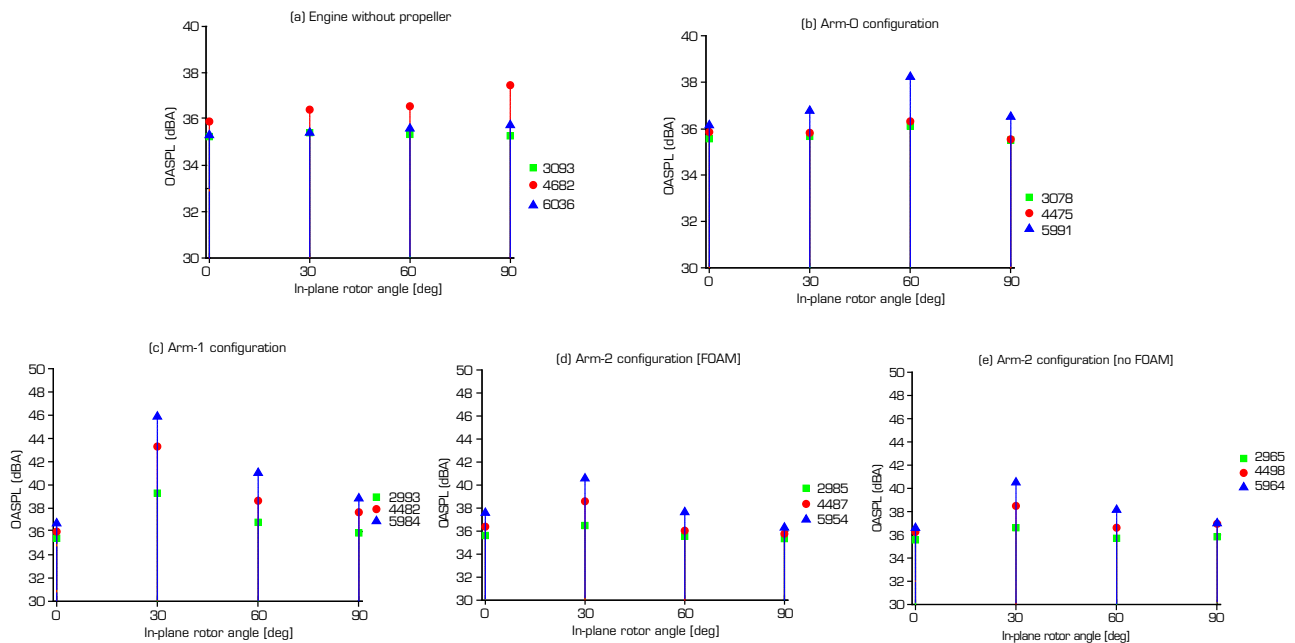
Figure 9 shows the sound profile plots, in terms of OASPL, from the in-plane receiver in the frequency domain for the four angles investigated. A comparison of OASPL, defined here as the summation of energy for the spectra obtained for the spectra, would indicate either a louder or a quieter configuration to the receiver. OASPLs are calculated over a frequency range of  $100 \leq f \leq 10$  kHz, focusing on lower frequencies dominated by the blade passing frequencies and harmonics.

The average sound profile plots indicated that the engine without propeller is reasonably below the values for the other configurations, except for rotational speeds close to 4,500 rpm. Arm-0 configuration presents a more uniform distribution of the sound for in-plane observer angles. Moreover, the noise levels were kept around and below 36 dBA. What is interesting to note is that for Arm-1, the noise levels scattered more for the angles 30° up to 60° with higher values. The noise levels for Arm-2 with and without insertion of foam were very similar.



Source: Elaborated by the authors.

**Figure 8.** Noise signature for the EA at different observer angles (0°, 30°, 60° and 90°).



Source: Elaborated by the authors.

**Figure 9.** Average sound profile (dBA) at different observer angles at 1 m high.

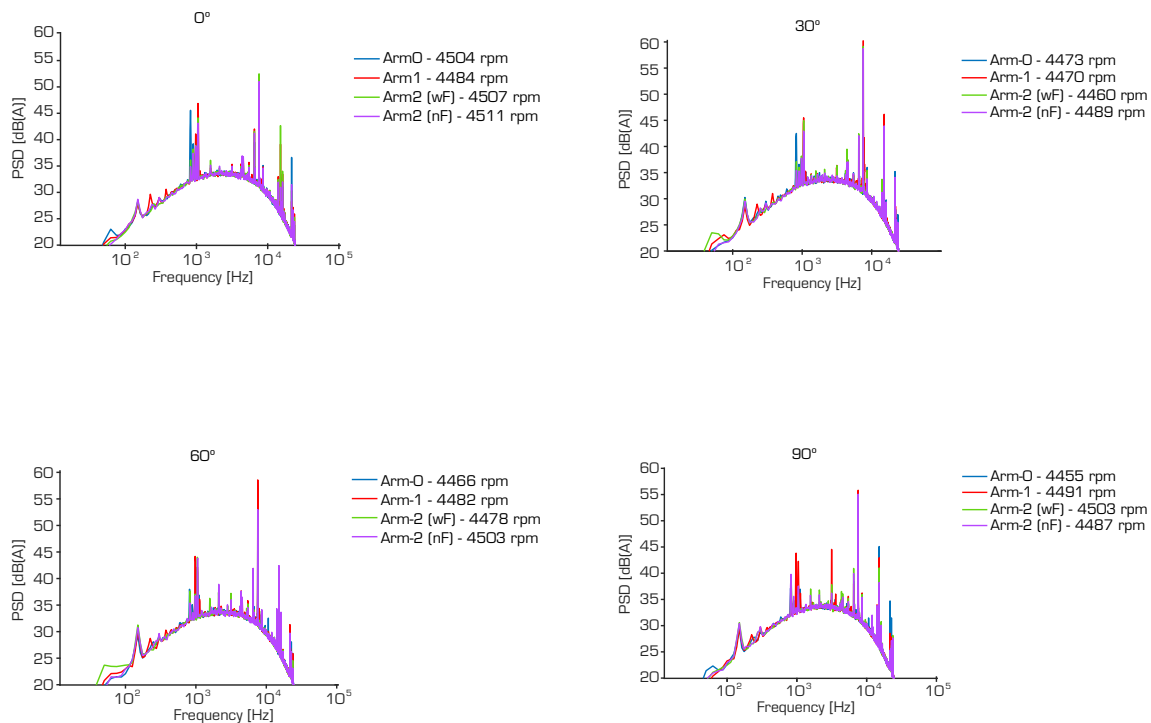
The analysis of the narrow-band spectra shows that the tonal components at very specific frequencies have pushed the OASPL values up to 38-40 dBA, scattering the noise as function of the receiver angle. In this sense, it is possible to verify that the noise signature is very sensitive to the geometry of the arm structure and receiver angle. Additional high intensity tonal peaks could be added to the final noise signature as a direct dependance of the geometrical design of the arm. However, it is worth mentioning that this study was conducted with only one rotor/structure and that the effects of multiple rotors must be taken into consideration when establishing the drone's acoustic signature. The following results will show the spectra for the effect



of the arm structure at 4,500 rpm operational setting, where it is possible to see the impact of the high intensity tonal peaks at medium and high frequency.

### Arm configuration effect at 4,500 rpm operation

By considering the maximum operation capability of the F450 and using as reference other works (Zarri *et al.* 2022), the default rotational speed to run the test would be of 4,500 rpm, that corresponds to a blade passage frequency (BPF) of 150 Hz. Figure 10 depicts the noise spectra by considering the different arm-configurations effects at 4,500 rpm.



Source: Elaborated by the authors.

**Figure 10.** A-weighted spectra for different arm-configuration as function of the receiver angles at 1 m high.

The obtained results did not provide a clear perspective on a significant noise improvement. Across the broadband spectrum, there seems to be an enhancement in both low and high frequencies, but this variation is angle dependent. Analyzing the interaction between the rotor and airframe is a highly complex task due to its strong dependence on other aerodynamic factors, such as blade loading, incoming turbulence, interaction between multiple rotors, vibroacoustics sources that may be present during the operation, etc.

Regarding Arm-1, it is evident that there are noticeable high-energy peaks in certain regions that do not appear in the results for the other arms. One possible explanation for this phenomenon could be attributed to the arm's cross-sectional shape resembling that of a droplet or an airfoil, which may generate vortices or turbulent residuals, leading to these pronounced energy spikes. Despite increasing the distance between the rotor and the arm in this scenario, improvements may be obscured by various aerodynamic factors. Another contributing factor is the surface finishing of the arm that did not undergo a more planned smoothing process, which may or may not have influenced the flow adherence to its surface. Nevertheless, the results were not entirely unsatisfactory. Some angles exhibited an improvement in broadband noise, and certain tonal peaks in both low and high frequencies remained consistent.

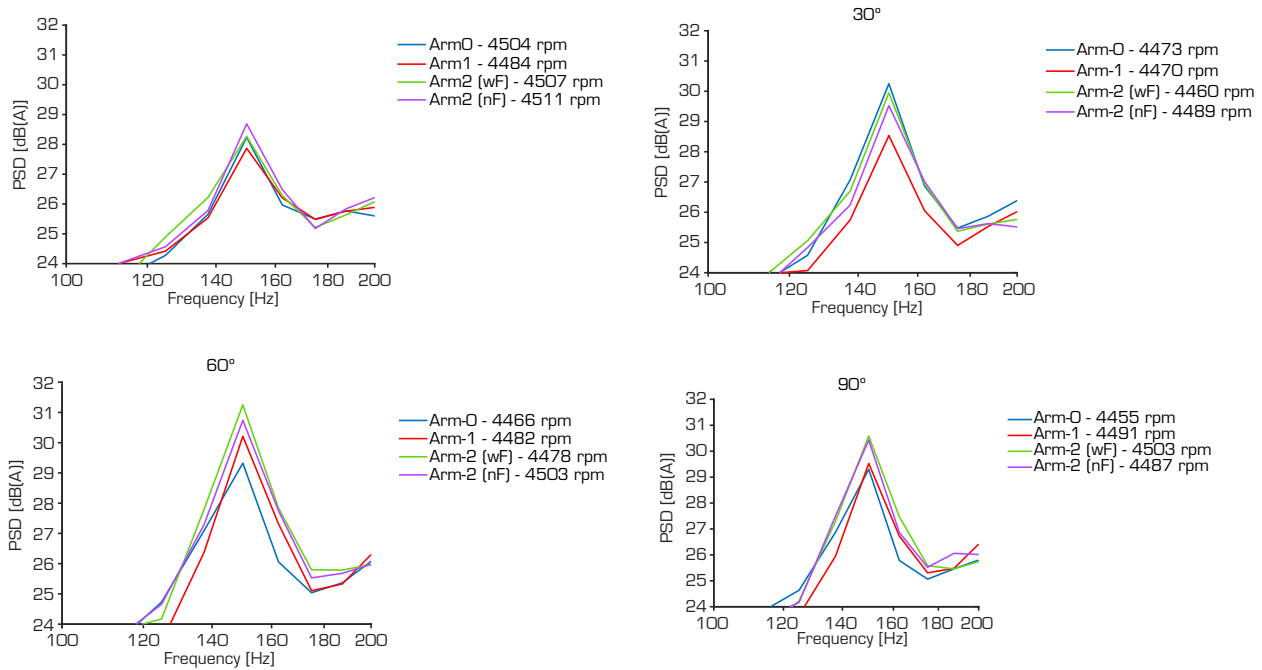
Continuing with Arm-2 (both with and without foam), the impact on attenuation or noise reduction appears to match the results observed in Arm-0, but the improvement fell short of expectations. Unlike Arm-1, there were no high-energy peaks in these two cases. However, the utilization of acoustic foam did not achieve noise attenuation levels superior to those of Arm-0.

Finally, it is important to emphasize the presence of tonal contents associated with the motor alone, as shown in Fig. 8. The motor alone helps to contribute to the level of tone and broadband noise in the mid [600-1,000 Hz] and high [7,500-15,000 Hz] frequency

range. The main discussion herein is that the aeroacoustics installation effects are due to the scattering of the sound radiated by the propeller and the airframe. As suggested by Zarri *et al.* (2022), acoustic installation effects due to scattering can strongly alter the acoustic emissions of a drone, with amplification or shielding effects.

As mentioned, some aspects indicate improvement in noise attenuation related to the blade passing frequency (BPF) as can be illustrated in the graphs in Fig. 11.

As depicted in the Fig. 10, the noise attenuation was indeed effective. Arm-1 demonstrated the highest level of noise reduction, achieving a decrease of 1.71 dBA. However, for the other angles, the reduction was either insignificant or, in some cases, showed no reduction at all.



Source: Elaborated by the authors.

**Figure 11.** Arm-configuration effect on BPF as function of the receiver angles at 1 m high.

## CONCLUSIONS

The focus of this study was to carry out acoustical research to discover possible methods for reducing the tonal noise generated by the interaction between the rotor and the airframe. Three distinct airframes for an F450 drone, which served as the focus of the study, were designed, and manufactured. An acoustical acquisition test was conducted to measure the varying pressure levels or noise levels experienced at four different positions (0°, 30°, 60°, and 90°) in the rotor-plane..

In conclusion, based on the data and results obtained, the projected arms showed a slight reduction in noise or attenuation in certain low and high frequencies. Arm-1 exhibited some high-energy tonal pulses, which may be attributed to aerodynamic effects resulting from its shape. In contrast, Arm-2, both with and without the foam, did not exhibit these high-energy pulses. As previously mentioned, due to the limited timeframe of this research, we were unable to analyze the aerodynamic behavior of the arms as originally planned.

Furthermore, it can be stated that the study yielded satisfactory results, recognizing that the aeroacoustics field is complex and relies on flow characterization for each specific problem. Numerous tests must be conducted before achieving a breakthrough or even a satisfactory outcome. One crucial aspect to consider in this work is that an aeroacoustics study must run concurrently

with an aerodynamic study. This is because turbulence itself generates noise, underscoring the importance of addressing both areas to mitigate this issue.

Although the arms did not outperform the default arm (Arm-0), they exhibited consistent behavior. In contrast, the noise A-weighting curves closely approximated the intended outcomes in this work, even in high frequencies, which are crucial for UAV operations. The noise production displayed coherency and, in some cases, attenuation. The maximum noise reduction observed in one of the comparisons was 1.71 dBA, suggesting that other reductions may have occurred, but were not explored or uncovered.

In future research, it would be valuable to delve into the aerodynamic aspects of this study, examining various configurations of airframes, different shapes, textures, depths of perforations, and use of sound absorbing materials.

## AUTHORS' CONTRIBUTION

**Conceptualization:** Almeida O and Sanchez GRL; **Methodology:** Almeida O and Sanchez GRL; **Software:** Almeida O and Sanchez GRL; **Validation:** Sanchez GRL; **Formal analysis:** Almeida O and Sanchez GRL; **Investigation:** Almeida O and Sanchez GRL; **Resources:** Almeida O and Catalano FM; **Data Curation:** Sanchez GRL; **Writing – Original Draft:** Sanchez GRL; **Writing – Review & Editing:** Almeida O; **Visualization:** Almeida O; **Supervision:** Almeida O; **Project administration:** Almeida. O; **Funding acquisition:** Almeida O and Catalano FM.


## CONFLICT OF INTEREST

Nothing to declare.

## DATA AVAILABILITY STATEMENT

All data sets were generated or analyzed in the current study.

## FUNDING

Financiadora de Estudos e Projetos   
Grant No: 0138/11

## ACKNOWLEDGEMENTS

Not applicable.

## REFERENCES

[AD] Airborne Drones (2020) Drone noise levels. [accessed Jan 13 2020]. <https://www.airbornedrones.co/drone-noise-levels/>

[EASA] European Union Aviation Safety Agency (2018) Introduction of a regulatory framework for the operation of unmanned aircraft systems in the 'open' and 'specific' categories. Opinion No.: 01/2018 2018.

- [FAA] Federal Aviation Administration (2022) FAA Aerospace Forecast, Fiscal Years 2019-2039. Washington, DC: FAA.
- [II] Insider Intelligence (2021) Drone technology uses and applications for commercial, industrial and military drones in 2021 and the future. [accessed Jul 12 2021]. <https://www.businessinsider.com/drone-technology-uses-applications>
- [ISO] International Organization for Standardization (1996) ISO 9613-2:1996 Acoustics – Attenuation of sound during propagation outdoors: Part 2: General method of calculation. Geneva: ISO. [accessed Oct 21 2020]. <https://www.iso.org/home.html>.
- [ISO] International Organization for Standardization (2003) ISO 226:2003: Acoustics – Normal equal-loudness-level contours. International Organization for Standardization. Geneva: ISO. [accessed Oct 21 2020]. <https://www.iso.org/home.html>.
- [NGS] National Geographic Society (2019) Noise pollution. Washington, D.C.: NGS. [accessed Jul 16 2019]. <https://www.nationalgeographic.org/encyclopedia/noise-pollution/>
- Brocklehurst A, Barakos GN (2013) A review of helicopter rotor blade tip shapes. *Prog Aerosp Sci* 56:35-74. <https://doi.org/10.1016/j.paerosci.2012.06.003>
- Candeloro P, Ragni D, Pagliaroli T (2022) Small-scale rotor aeroacoustics for drone propulsion: a review of noise sources and control strategies. *Fluids* 7(8):279. <https://doi.org/10.3390/fluids7080279>
- Caprace DG, Ning A, Chatelai P, Winckelmans G (2022) Effects of rotor-airframe interaction on the aeromechanics and wake of a quadcopter in forward flight. *Aerosp Sci Technol* 130:107899. <https://doi.org/10.1016/j.ast.2022.107899>
- Intaratep N, Alexander WN, Devenport WJ, Grace SM, Dropkin A (2016) Experimental study of quadcopter acoustics and performance at static thrust conditions. Paper presented 22nd AIAA/CEAS Aeroacoustics Conference. AIAA/CEAS; Lyon, France. <https://doi.org/10.2514/6.2020-2595>
- Jordan WA, Narsipur S, Deters R (2020) Aerodynamic and aeroacoustic performance of small UAV propellers in static conditions. Paper presented 2020 AIAA Aviation Forum. AIAA (virtual conference in an online-only format). <https://doi.org/10.2514/6.2020-2595>
- Kekus-Kumor P, Sieradzki A (2023). Experimental investigation of unmanned air vehicle rotor aeroacoustics using benchmark geometries. Paper presented INTER-NOISE and NOISE-CON Congress and Conference Proceedings. Institute of Noise Control Engineering; Chiba, Japan. [https://doi.org/10.3397/IN\\_2023\\_0769](https://doi.org/10.3397/IN_2023_0769)
- Kloet N, Watkins S, Clothier R (2017) Acoustic signature measurement of small multi-rotor unmanned aircraft systems. *Int J Micro Air Veh* 9(1):3-14. <https://doi.org/10.1177/1756829316681868>
- Lee H, Lee DJ (2020) Rotor interactional effects on aerodynamic and noise characteristics of a small multirotor unmanned aerial vehicle. *Phys Fluids* 32: 047107. <https://doi.org/10.1063/5.0003992>
- Molino JA (1982) Should helicopter noise be measured differently from other aircraft noise? A review of the psychoacoustic literature. Arlington: NASA.
- Oleson R, Patrick H (1998) Small aircraft propeller noise with ducted propeller. Paper presented 4th AIAA/CEAS Aeroacoustics Conference. AIAA/CEAS; Toulouse, France. <https://doi.org/10.2514/6.1998-2284>
- Roger M (2019) Aeroacoustics of installed propellers. von Karman Institute Lecture Series. Vol. 2019-02. Sint-Genesius-Rode: von Karman Institute for Fluid Dynamics.
- Wang Z, Henricks Q, Zhuan M, Pandey A, Sutkowsky M, Harter B, McCrink M, Gregory J (2019) Impact of rotor-airframe orientation on the aerodynamic and aeroacoustic characteristics of small unmanned aerial systems. *Drones* 3(3):56. <https://doi.org/10.3390/drones3030056>

Watkins S, Burry J, Mohamed A, Marino M, Prudden S, Fisher A, Kloet N, Jakobi T, Clothier R (2020) Ten questions concerning the use of drones in urban environments. *Build Environ* 167:106458. <https://doi.org/10.1016/j.buildenv.2019.106458>

Whelchel J, Alexander WN (2021) sUAS rotor-airframe interaction. Paper presented AIAA Aviation 2021 Forum. AIAA (virtual conference in an online-only format). <https://doi.org/10.2514/6.2021-2212>

Zarri A, Dell'Erba E, Munters W, Schram C (2022) Aeroacoustic installation effects in multi-rotorcraft: numerical investigations of a small-size drone model. *Aerosp Sci Technol* 128:107762. <https://doi.org/10.1016/j.ast.2022.107762>

Zawodny N, Pettingill N, Thurman C (2023) Identification and reduction of interactional noise of a quadcopter in hover and forward flight conditions. Paper presented INTER-NOISE and NOISE-CON Congress and Conference Proceedings. Institute of Noise Control Engineering; Glasgow, Scotland. [https://doi.org/10.3397/IN\\_2022\\_0415](https://doi.org/10.3397/IN_2022_0415)

Zawodny NS, Christian A, Cabell R (2018) A summary of NASA research exploring the acoustics of small unmanned aerial systems. Paper presented 2018 AHS Technical Meeting on Aeromechanics Design for Transformative Vertical Flight. American Helicopter Society International; San Francisco, USA.